Measurement and calculation of transmission neutron spectra from 238U induced by broad-spectrum neutrons

Authors: Sun, Dr. Hui, Zhang, Dr. Xin, Zhi-Qiang Chen, Han, Miss Rui, YANG, Dr. Bo, Khasanov, Mr. Shakhboz, Zhang, Dr. Peiyan Zhang Peiyan, Tian, Dr. Guoyu, Liu, Dr. Bing-Yan, Shi, Mr. Fudong, Zhang, Ze-Kun, Li, Mr. Qin, LUO, Dr. PENG, Sun, Dr. Hui

Date: 2025-09-30T20:26:10+00:00

Abstract

Transmission neutron spectra from a pure 238U slab sample (dimensions: 100 mm × 100 mm × 20 mm) bombarded by broad-spectrum neutrons were measured at 0° using the time-of-flight method. The experiment was carried out at the Radioactive Ion Beam Line of the Heavy Ion Research Facility in Lanzhou at the Institute of Modern Physics, Chinese Academy of Sciences. Broad-spectrum neutrons were generated by bombarding a tungsten target with 80.5 MeV/u 12C ions. Additionally, calculations were performed in GEANT4 with the INCL, BIC and BERT physics models, in combination with the evaluated nuclear data libraries ENDF/BVIII, JEFF-3.3, and JENDL-4.0, and the theoretical results for the transmission neutron spectrum of the 238U were obtained under the same experimental conditions. The results indicate that the GEANT4 calculations can reasonably reproduce the experimental data.

Full Text

Measurement and Calculation of Transmission Neutron Spectra from 238U Induced by Broad-Spectrum Neutrons

Hui Sun,[1,2,†] Xin Zhang,[1,2] Zhi-Qiang Chen,[1,2,3] Rui Han,[1,2,3,‡] Bo Yang,[1] Shakhboz Khasanov,[4] Pei-Yan Zhang,[1,3] Guo-Yu Tian,[1,2] Bing-Yan Liu,[1,2] Fu-Dong Shi,[1,2] Ze-Kun Zhang,[1,3] Qin Li,[1,3] and Peng Luo[1,2,3]

[1]Institute of Modern Physics, Chinese Academy of Sciences, Lanzhou 730000, China
[2]Gansu Isotope Laboratory, Lanzhou, 730300, China

[3]School of Nuclear Science and Technology, University of Chinese Academy of Sciences, Beijing 100049, China
[4]Samarkand State University, Samarkand 140104, Uzbekistan

Transmission neutron spectra from a pure 238U slab sample (dimensions: 100 mm × 100 mm × 20 mm) bombarded by broad-spectrum neutrons were measured at 0° using the time-of-flight method. The experiment was carried out at the Radioactive Ion Beam Line of the Heavy Ion Research Facility in Lanzhou at the Institute of Modern Physics, Chinese Academy of Sciences. Broad-spectrum neutrons were generated by bombarding a tungsten target with 80.5 MeV/u 12C ions. Additionally, calculations were performed in GEANT4 with the INCL, BIC and BERT physics models, in combination with the evaluated nuclear data libraries ENDF/B-VIII.0, JEFF-3.3, and JENDL-4.0, and the theoretical results for the transmission neutron spectrum of the 238U were obtained under the same experimental conditions. The results indicate that the GEANT4 calculations can reasonably reproduce the experimental data.

Keywords: Transmission neutron spectra, 238U, Broad-spectrum neutrons, GEANT4

INTRODUCTION

The Accelerator-Driven System (ADS) is a coupled system comprising a subcritical reactor and an external proton accelerator [1–3]. The system possesses strong transmutation capabilities, significant neutron economy, and reliable safety performance. Not only can it convert spent nuclear fuel into short-lived isotopes, but it also has the potential to both proliferate nuclear fuel and generate electricity in an efficient and sustainable manner [4, 5]. Therefore, the ADS exhibits favorable energy economics and is an important research area within the field of nuclear energy [6–12]. The advancement of ADS is currently at a critical stage of technological development [13], necessitating substantial support from nuclear data resources [14–17].

In the ADS, the secondary neutrons generated by beam-induced spallation reactions are characterized by high flux and broad energy spectrum. These neutrons not only serve as the primary driver for spent fuel transmutation, but the transmitted neutrons also constitute the most critical radiation source term in shielding design. Therefore, investigating neutron transport processes in relevant materials is crucial for the design of core structure, target-core coupling, and radiation shielding. Monte Carlo codes based on established physical models and evaluated nuclear data libraries are fundamental tools for conducting neutron transport simulations. The iterative optimization of subcritical system parameters—including geometric configuration and material selection—using accurate physical models and evaluated databases is of significant importance for enhancing neutron yield and utilization efficiency, reducing neutron loss, improving neutron flux management in subcritical cores, accurately predicting core temperature distributions under various operational conditions, and achieving

optimal radiation protection.

238U is a critical nuclear material for ADS, and the neutron transport nuclear data of 238U form an important foundation for both the ADS and advanced nuclear fuel cycle systems [17–20]. However, significant discrepancies exist among the evaluated neutron data for 238U within the energy range below 20 MeV, and such data are notably scarce in the medium and high-energy ranges [21–26]. At present, the existing neutron evaluation data for 238U are difficult to directly apply under the complex conditions of high neutron flux and broad energy spectrum encountered in ADS. Therefore, there is a critical need for detailed and reliable experimental measurements as well as theoretical calculations concerning the relevant nuclear data of the interaction between medium- and high-energy neutrons with 238U.

238U is an extremely critical nuclear material for the Accelerator-Driven System. The content of 238U in spent nuclear fuel is more than 95 percent, and the proportion of reactions involving spallation neutrons and 238U within the reactor core is high, and these reactions are notably complex. The neutron transport processes in 238U serve as an essential basis for ADS [17, 20]. After capturing a neutron, 238U can be transformed into a fissionable nuclide, 239Pu (238U + n → 239U → 239Np → 239Pu fissile) [18, 27]. The recycling of 238U through the uranium-plutonium cycle plays a significant role in enhancing the disposal capacity for spent nuclear fuel and promoting the efficiency of the nuclear fuel cycle. This is also an important means to achieve the sustainable development of nuclear fission energy. In addition, the complex reactions between broad-spectrum neutrons and 238U will affect the neutron characteristics in the spallation target region.

In this work, we utilized 12C + W as the neutron source. The transmission neutron spectrum is measured by time-of-flight method, by bombarding the 238U sample target with broad-spectrum neutrons. Moreover, GEANT4 [28] is used to simulate the experimental process in combination with the INCL++ [29], BIC [30] and BERT [31, 32] physical models and the ENDF/B-VIII.0 [33], JEFF-3.3 [34] and JENDL-4.0 [35] evaluation databases.

METHODS

A. Experimental Methodology

The experiment was carried out at the Radioactive Ion Beam Line in Lanzhou (RIBLL) [36, 37]. The primary beam was 80.5 MeV/u 12C delivered by the Heavy Ion Research Facility in Lanzhou (HIRFL) [38, 39], located at the Institute of Modern Physics, Chinese Academy of Sciences.

Fig. 1 shows the layout diagram of the neutron source experimental device. In this work, the broad-spectrum neutrons generated by this setup served as source neutrons, interacting with a 238U target sample. The resulting transmission neutron spectrum was then measured. The 12C ions were accelerated to

an energy of 80.5 MeV/u and focused onto a natural tungsten cylinder target (dimensions: 50 mm × 5 mm). The tungsten target was attached to the exit window, which was made of a 3-mm-thick iron plate at the end of the vacuum chamber. The bombardment of the tungsten target by the 12C beam generates a large number of secondary particles, including neutrons, gamma rays, protons, deuterons, tritons, and 3He nuclei. These secondary particles can penetrate through the target medium and the surrounding air, allowing their signals to be detected by the detectors (EJ212 and BC501A).

Fig. 2 shows the layout diagram of the experimental device for the transport of broad-spectrum neutrons in the 238U target (dimensions: 100 mm × 100 mm × 20 mm; thickness along the neutron penetration direction: d = 20 mm; purity: p = 99.9 %; density: = 18.79 g/cm^3). In this experiment, the time-of-flight method was employed to measure the transmission neutron spectrum. As shown in the figure, the experimental device is largely consistent with that of the neutron source facility (Fig. 1). The difference is that the plastic scintillation detector (Veto) and the 238U target are placed on the outer side of the vacuum chamber. The Veto is used to remove the effects of charged particles on the transmission neutron spectrum during data analysis. The beam pickup detector (TP, a plastic scintillator detector) positioned within the vacuum chamber is located 67 cm upstream of the tungsten target. During the experiment, the TP served to monitor beam parameters, provide timing information for the beam and count incident particles, while also acting as the stop signal for neutron time-of-flight measurements. Additionally, 12C ions were fully deposited in the primary target (tungsten target), with their range calculated using LISE++ being equal to 1.912 mm.

In this experiment, the detection system consisted of an EJ212 plastic scintillator detector (Veto) and a BC501A liquid scintillator detector (N1). This system allowed effective discrimination between charged and neutral particles. After removing signals due to charged particles, the remaining spectrum enabled differentiation between neutron and gamma signals detected by the liquid scintillator via pulse shape discrimination (PSD), as shown in Fig. 3. The BC501A liquid scintillator detector primarily consists of a cylindrical liquid scintillator crystal, an optical collection system, a photomultiplier tube, and a voltage divider. The liquid scintillator crystal inside the BC501A probe has a diameter and length of 12.7 cm each, a maximum emission wavelength of 425 nm, and an emission decay time of approximately 3.2 ns. The EJ212 plastic scintillation detector is a rectangular cuboid with dimensions of 12.7 cm × 12.7 cm × 5 mm and has a square cross-section facing the incident beam direction. Its distinguishing characteristic is a very low probability of interaction with neutral particles, while it exhibits high sensitivity to charged particles.

B. Electronics and Data Acquisition

Fig. 4 shows a schematic diagram of the electronics and data acquisition system employed in the neutron transport experiment for 238U. As shown in the

figure, the signal from the beam pickup detector (TP or BM) located in the target chamber is divided into four channels. The signal from Channel 1 is fed into a Charge-Integrating Digital Converter (QDC) to record beam energy information. The signal from Channel 2 is processed by a Constant Fraction Discriminator (CFD) and then fed into a Time-to-Digital Converter (TDC) to serve as the stop signal for neutron time-of-flight measurement. The signal from Channel 3 passes through the CFD and enters the Scaler. The signal from Channel 4 is processed by the CFD and then directed to a Logic Coincidence Unit (Coin), where it is used in coincidence with the output signal from the neutron detector to identify true nuclear reaction events. This coincident signal is subsequently sent to the Scaler and also serves as the electronics trigger signal (Trigger) for the entire experiment. Signals from the plastic scintillator detectors (Veto1 and Veto2) are directly input to the QDC for removing charged particle events during data analysis. The output signal from the liquid scintillator detector (BC501A) is split into three channels as illustrated: The Channel 1 signal is processed by the CFD and then fed into the TDC to serve as the start time for neutron time-of-flight measurement; The Channel 2 signal is used for fast/slow component discrimination in the QDC; The Channel 3 signal passes through the CFD and is then input to the coincidence unit for coincidence measurement with the BM signal.

C. Monte Carlo Calculation

GEANT4 is a versatile Monte Carlo software toolkit for the calculation of the passage of particles through matter. It is widely used across various fields, including high-energy physics, accelerator physics, astrophysics and space science, medical physics and radiation protection. GEANT4 provides a variety of physical models describing the interaction between particles and nuclei, along with comprehensive lists of associated models for users to utilize, such as BERT (Bertini intranuclear cascade model), BIC (Binary cascade model), and INCL++ (Intranuclear cascade liege). BERT integrates the Bertini intranuclear cascade model, pre-equilibrium model, fission model, and evaporation model. It is capable of simulating nuclear reactions induced by long-lived hadrons and gamma rays with energies up to 10 GeV. BIC simulates the cascade transport process of primary and secondary particles within the nucleus. It only considers the two-body interactions between primary or secondary particles and individual nucleons within the nucleus. INCL++ is applicable for simulating particle bombardment of target nuclei heavier than deuterium within the energy range of 1 MeV/u to 20 GeV/u. However, its applicability to light and unstable nuclei has not yet been comprehensively validated.

In order to verify the reliability of GEANT4 in the transport calculation process, this study employs “Geant4-10.7.4” to simulate the experimental process in combination with the INCL++, BIC and BERT physical models and the ENDF/B-VIII.0, JEFF-3.3 and JENDL-4.0 evaluation databases. The resulting transmission neutron spectra are obtained under the same experimental

conditions.

DATA ANALYZING PROCEDURE

A. Neutron Energy Calculation

The time-of-flight (TOF) method for measuring neutron energy spectra is based on the principle that neutrons with different energies require different amounts of time to travel the same distance. It is a measurement technique that calculates neutron energy based on the known flight distance and corresponding travel time, and it is now widely used in neutron experiment measurements [40–43].

In this experiment, the flight distance L is defined as the distance between the center of the target sample and the geometric center of the detector. It should be noted that since the beam pickup detector is positioned at a certain distance upstream from the target, the time difference between the trigger signal and the stop signal cannot be directly used as the neutron time of flight. The actual neutron time of flight is obtained by taking the time difference between the neutron peak and the gamma peak in the TOF spectrum, plus the flight time of the gamma rays from the target center to the detector center. Fig. 5 displays the time-of-flight spectra of neutrons and gamma rays, with the charged-particle background removed. The neutron energy can then be derived from the TOF spectrum using the following Eq. (1):

$$E = ((\text{cid:113})1 - (\Delta Tc + L) - 1)m_{nc}^2$$

where E is the energy of the neutron, L is the flight distance from the center of the target to the geometric center of the detector, ΔT is the difference of flight times between the prompt gamma ray and the neutron, c is the velocity of light in a vacuum, and m is the rest mass of the neutron.

B. Energy Calibration and Neutron-Detection Efficiency

The energy calibration results of the neutron detector directly affect the accuracy and reliability of the transmission neutron spectrum. Therefore, the energy calibration of the detector is of vital importance in neutron transport experiments. Based on the principle that the light output of low-energy electrons in the liquid scintillator detector is linearly related to the electron energy, standard gamma-ray sources (^{137}Cs, ^{60}Co, and ^{22}Na) were used to calibrate the energy of the BC501A (N1) detector. The energy calibration results are shown in Fig. 6.

The detection efficiency ( ) is defined as the ratio of the number of detected particles to the number of particles incident on the detector. Due to the limitations imposed by detector type, geometric dimensions, energy threshold, the type and energy of the incident particles, as well as the dead time of the data acquisition system, not all neutrons entering the detector can be recorded. To obtain a

more accurate neutron transmission spectrum, the neutron detection efficiency must therefore be determined. In this experiment, the SCINFUL-QMD [44, 45] simulation program was used to calculate the detection efficiency of the liquid scintillator detector under different detection thresholds. When the neutron energy is below 80 MeV, the software employs the SCINFUL model for calculations; for energies above 80 MeV but below 3 GeV, it utilizes the Quantum Molecular Dynamics (QMD) model and the Statistical Decay Model (SDM) for calculations. In previous work, the software has been benchmarked and applied to neutron transport experiments. The result is shown in Fig. 7.

C. Experimental Background

Background neutron measurements were conducted to evaluate the background contribution of scattered neutrons in the experimental hall. Fig. 8 shows the experimental setup for measuring scattered background neutrons. A shadow bar made of iron, measuring 15 cm × 15 cm in cross-section and 100 cm in length, was placed along the flight path from the target to the liquid scintillator detector. This setup blocked almost all direct neutrons, allowing only the scattered components to reach the neutron detector. Fig. 9 displays the time-of-flight spectrum of the background neutrons.

D. Uncertainty and Energy Resolution

The uncertainty of the experimental data consists of statistical and systematic errors. The statistical error was less than 5% at energies below 20 MeV and increased to 35% at higher energies from the neutron counts. The systematic error arises mainly from uncertainties in the detection efficiency calculation, being less than 10% for incident neutron energies in the range of 0.1–80 MeV and approximately 15% for higher-energy neutrons. The energy resolution can be expressed by the following Eq. (2):

$$\frac{\Delta E}{E} = \Upsilon(\Upsilon + 1)\frac{\Delta t}{t}$$

where Υ is the Lorentz factor, ΔT is the difference in flight times between the prompt gamma ray and the neutron. The time resolution Δt was estimated to be 1.5 ns which is obtained from the Full Width at Half Maximum (FWHM) of the prompt gamma-ray peak, as shown in Fig. 5.

RESULTS AND DISCUSSION

In this experiment, broad-spectrum neutrons emitted from a 5 mm-thick tungsten target bombarded by 80.5 MeV/u 12C ions were measured using the time-of-flight method. Subsequently, the transmission neutron spectrum at 0° was measured from the interaction of these broad-spectrum neutrons with a 238U target. Parallel calculations were performed using GEANT4 with the INCL++,

BIC and BERT physics models, combined with the ENDF/B-VIII.0, JEFF-3.3 and JENDL-4.0 evaluated databases. The transmission neutron spectrum under identical experimental conditions was thereby obtained through these calculations.

Fig. 10 compares the transmission neutron spectrum of the 238U target with the source neutron spectrum (i.e., the broad-spectrum neutrons generated by 12C bombardment of the W target). In the figure, the blue solid squares represent the source neutron spectrum. The red solid circles show the transmission neutron spectrum at 0° after the source neutrons transported through the 238U target. The results indicate that the 20 mm-thick 238U target affects neutrons across the entire studied energy range, with a more pronounced influence observed for neutrons below 50 MeV.

Fig. 11 shows a comparison between experimental data and GEANT4 calculation results for the transmission neutron spectrum of the 238U target at the 0° direction. The solid black dots represent the experimental results obtained in this study, while lines in other colors (red, green, and blue) correspond to different physics models (INCL++, BIC, and BERT). The solid lines, dashed lines, and dash-dotted lines respectively represent different evaluated databases (ENDF/B-VIII.0, JEFF-3.3, and JENDL-4.0). It can be observed in Fig. 11 that the GEANT4 simulation results agree well with the experimental data. Fig. 12 presents the ratio between the calculated and experimental values. As is shown in the figure, within the 20–70 MeV energy range, the results from all three models agree well with the experimental data, with a discrepancy not exceeding 15%. Above 70 MeV, the errors in the calculation results of all three models increase, with a clear underestimation of the experimental data. Overall, for the transport of broad-spectrum neutrons in 238U, GEANT4 combined with the three aforementioned physics models yields reasonably good agreement with experimental data in the energy range above 20 MeV. Nevertheless, the description deteriorates in the higher energy region, indicating that the high-energy models still require further optimization.

Since GEANT4 utilizes evaluated databases for calculations in the energy range below 20 MeV, a separate comparison between experimental measurements and calculation results for the transmission neutron spectrum below 20 MeV is presented in Fig. 13 to highlight differences among the databases. A combined analysis of Fig. 12 and 13 reveals that: below 20 MeV, the differences in results obtained by invoking different evaluated databases (ENDF/B-VIII.0, JEFF-3.3 and JENDL-4.0) are very small for the same physical model. This is because the evaluated databases are well-established and show little variation in this energy region. However, below 10 MeV, a significant discrepancy emerges between the theoretical calculations and the experimental data. All the calculation results collectively overestimate the experimental data. Besides, the BERT model yields higher results than INCL++ and BIC in this low-energy range (below 10 MeV). Above 10 MeV, the results from all three models show good agreement.

CONCLUSIONS

The experiment described in this paper was carried out at the Radioactive Ion Beam Line in Lanzhou (RIBLL). The time-of-flight (TOF) method was employed to measure the transmission neutron spectrum at 0° generated by the interaction of the broad-spectrum neutrons (high-energy white-light neutrons) with a 238U target. Additionally, calculations were performed using GEANT4 combined with the INCL++, BIC, and BERT physics models, as well as the evaluated nuclear data libraries ENDF/B-VIII.0, JEFF-3.3, and JENDL-4.0. Under the same experimental conditions, the theoretical results for the transmission neutron spectrum were obtained.

The results indicate that the calculations using the three physical models combined with different evaluated nuclear data libraries all accurately reproduced the experimental data. However, slight overestimations were observed below 10 MeV when these models were paired with different data libraries. Overall, GEANT4 demonstrates reliable calculations for the transport process of high-energy neutrons in 238U targets.

This work fills a gap in the studies of high-energy neutron transport for the 238U target. The reliable transport experimental data provide valuable reference information for the design and construction of ADS projects. Additionally, the study examines the reliability of the evaluated databases and theoretical models in the GEANT4 program, and contributes to model improvement and the refinement of evaluated databases, which is of significant importance.

ACKNOWLEDGEMENTS

The authors would like to express sincere thanks to the staffs of the Heavy Ion Research Facility in Lanzhou for their excellent operation of the accelerator and assistance during the irradiation.

AUTHOR CONTRIBUTIONS

All authors contributed to the study conception and design. Material preparation, data collection and analysis were performed by Hui Sun, Xin Zhang and Rui Han. Theoretical calculation and analysis were performed by Hui Sun and Zhi-Qiang Chen. The project was leaded and supervised by Zhi-Qiang Chen, Rui Han and Hui Sun. The first draft of the manuscript was written by Hui Sun, and all authors commented on previous versions of the manuscript. All authors read and approved the final manuscript.

REFERENCES

[1] B. Yee-Rendon, Overview of ADS projects in the world. *Int. Linear Accel. Conf.* 31, 310–313 (2022). doi:10.18429/JACoW-LINAC2022-TU2AA01

[2] A. Rummana, R. J. Barlow, S. M. Saad, et al., Calculations of neutron fluxes and isotope conversion rates in a thorium-fuelled MYRRHA reactor, using GEANT4 and MCNPX. *Nucl. Eng. Des.* 388, 111629 (2022). doi:10.1016/j.nucengdes.2021.111629

[3] C. H. Pyeon, Accelerator-Driven System at Kyoto University Critical Assembly. Osaka, Japan. 13–345 (2021). doi:10.1007/978-981-16-0344-0

[4] X. Y. Sun, W. Luo, H. Y. Lan, et al., Transmutation of long-lived fission products in an advanced nuclear energy system. *Sci. Rep.* 12, 2240 (2022). doi:10.1038/s41598-022-06344-y

[5] X. Yan, L. Yang, X. Zhang, et al., Concept of an Accelerator-Driven Advanced Nuclear Energy System. *Journal. Energies.* 10, 944 (2017). doi:10.3390/en10070944

[6] A. Rummana, R. J. Barlow, Simulation and parameterisation of spallation neutron distributions. *Proceedings of Science.* 32 (2017). doi:10.22323/1.279.0023

[7] A. I. Dubrouskia, A. I. Kiyavitskayaa, Simulation of Neutronics of an Accelerator Driven System. *Phys. Part. Nuclei Lett.* 17, 19–26 (2020). doi:10.1134/S1547477120010069

[8] H. Meng, Y. Yang, Z. Zhao, et al., Physical studies of minor actinide transmutation in the accelerator-driven subcritical system. *Nucl. Sci. Tech.* 30, 95–103 (2019). doi:10.1007/s41365-019-0453-9

[9] A. Al Qaaod, V. Gulik, 226Ra irradiation to produce 225Ac and 213Bi in an accelerator-driven system reactor. *Nucl. Sci. Tech.* 31, 14–19 (2020). doi:10.1007/s41365-020-00753-2

[10] L. Zhang, S. Chen, Z, Zhang, et al., Resolution analysis of thermal neutron radiography based on accelerator-driven compact neutron source. *Nucl. Sci. Tech.* 34, 143–155 (2023). doi:10.1007/s41365-023-01227-x

[11] X. Zhao, D. Cui, X. Cai, et al., Analysis of Th-U breeding capability for an accelerator-driven subcritical molten salt reactor. *Nucl. Sci. Tech.* 29, 119–127 (2018). doi:10.1007/s41365-018-0466-0

[12] L. Yang, W. Zhan, A closed nuclear energy system by accelerator-driven ceramic reactor and extend AIROX reprocessing. *Science China(Technological Sciences).* 60, 1702–1706 (2017). doi:10.1007/s11431-017-9089-0

[13] W. M. Pan, Overview of worldwide accelerators for ADS. *Int. Part. Accel. Conf.* 5, 4069–4072 (2014). doi:10.18429/JACoW-IPAC2014-FRXCB01

[14] S. Ganesan, Nuclear data requirements for accelerator driven sub-critical systems – A roadmap in the Indian context. *Pramana - J Phys.* 68, 257–268 (2007). doi:10.1007/s12043-007-0111-7

[15] A. Stankovskiya, Y. Çelik, G. V. Eynde, Impact of intermediate and high energy nuclear data on the neutronic safety parameters of MYRRHA accelerator driven system. *EPJ Web of Conferences.* 146, 09001 (2017). doi:10.1051/epjconf/201714609001

[16] A. Stankovskiy, H. Iwamoto, Y. Çelik, et al., High-energy nuclear data uncertainties propagated to MYRRHA safety parameters. *Ann. Nucl. Energy.* 120, 207–218 (2018). doi:10.1016/j.anucene.2018.05.041

[17] R. Asiya, Spallation Neutron Source for an Accelerator Driven Subcritical Reactor. Doctoral thesis, University of Huddersfield. 1–123 (2019). doi:eprints.hud.ac.uk/id/eprint/35075/

[18] P. K. Nema, Application of Accelerators for Nuclear Systems: Accelerator Driven System (ADS). *Energy Procedia.* 7, 597–608 (2011). doi:10.1016/j.egypro.2011.06.080

[19] Q. Sun, Z. Chen, R. Han, et al., Experiment on uranium slabs of different thicknesses with D-T neutrons and validation of evaluated nuclear data. *Fusion Eng. Des.* 125, 9–17 (2017). doi:10.1016/j.fusengdes.2017.10.021

[20] P. Vaz, Neutron transport simulation. *Radiat. Phys. Chem.* 78, 829–842 (2009). doi:10.1016/j.radphyschem.2009.04.022

[21] Y. Zhang, R. Xu, Y. Tian, et al., Evaluations and calculations of neutron reactions on 238U up to 20 MeV. *Nucl. Eng. Technol.* 57, 103190 (2025). doi:10.1016/j.net.2024.08.059

[22] Z. Yuan, S. Shen, X. Luo, Measurement of the 238U(n,γ)239U reaction cross sections in the energy range of 2.0–5.0 MeV by using a neutron activation technique. *J. Radioanal. Nucl. Chem.* 324, 277–283 (2020). doi:10.1007/s10967-020-07046-3

[23] A. M. Daskalakis, R. M. Bahran, E. J. Blain, et al., Quasi-differential neutron scattering from 238U from 0.5 to 20 MeV. *Ann. Nucl. Energy.* 73, 455–464 (2014). doi:10.1016/j.anucene.2014.07.023

[24] Y. Nie, J. Bao, X. Ruan, et al., Benchmarking of evaluated nuclear data for uranium by a 14.8 MeV neutron leakage spectra experiment with slab sample. *Ann. Nucl. Energy.* 37, 1456–1460 (2010). doi:10.1016/j.anucene.2010.06.018

[25] Y. Ding, Y. Nie, Y. Zhang, et al., Benchmark experiment on slab 238U with D-T neutrons for validation of evaluated nuclear data. *Nucl. Sci. Tech.* 35, 29 (2024). doi:10.1007/s41365-024-01409-8

[26] Q. Wang, T. Liu, Y. Qiu, et al., Measurement of the cross sections for 238U(n,γ)239U reaction in the energy range of 14.1–14.8 MeV using neutron activation method. *Radiat. Phys. Chem.* 152, 125–128 (2018). doi:10.1016/j.radphyschem.2018.08.013

[27] Z. Yuan • S. Shen • X. Luo, et al., Molten salt fast reactor with U–Pu fuel cycle. *Prog. Nucl. Energy.* 82, 33–36 (2015). doi:10.1016/j.pnucene.2014.07.014

[28] J. Allison, K. Amako, J. Apostolakis, et al., Recent developments in GEANT4. *Nucl Instrum Meth A.* 835, 186–225 (2016). doi:10.1016/j.nima.2016.06.125

[29] D. Mancusi, A. Boudard, J. Cugnon, et al., Extension of the Liège intranuclear-cascade model to reactions induced by light nuclei. *Phys. Rev. C.* 90, 054602 (2014). doi:10.1103/PhysRevC.90.054602

[30] G. Folger, V. N. Ivanchenko, J. P. Wellischa, The Binary Cascade Nucleon nuclear reactions. *Eur. Phys. J. A.* 21, 407–417 (2004). doi:10.1140/epja/i2003-10219-7

[31] H. W. Bertini, M. P. Guthrie, News item results from medium-energy intranuclear-cascade calculation. *Nucl. Phys. A.* 169, 670–672 (1971). doi:10.1016/0375-9474(71)90710-X

[32] M. P. Guthrie, R. G. Alsmiller Jr., H. W. Bertini, Calculation of the capture of negative pions in light elements and comparison with experiments pertaining to cancer radiotherapy. *Nucl. Instr. and Meth.* 66, 29–36 (1968). doi:10.1016/0029-554X(68)90054-2

[33] D. A. Brown, M. B. Chadwick, R. Capote, et al., ENDF/B-VIII.0: The 8th Major Release of the Nuclear Reaction Data Library with CIELO-project Cross Sections, New Standards and Thermal Scattering Data. *Nucl. Data Sheets.* 148, 1–142 (2018). doi:10.1016/j.nds.2018.02.001

[34] A. J. M. Plompen, O. Cabellos, C. De Saint Jean, et al., The joint evaluated fission and fusion nuclear data library, JEFF-3.3. *Eur. Phys. J. A.* 56, 181 (2020). doi:10.1140/epja/s10050-020-00130-2

[35] K. Shibata, O. Iwamoto, T. Nakagawa, et al., JENDL-4.0: A New Library for Nuclear Science and Engineering. *J. Nucl. Sci. Technol.* 48, 1–30 (2011). doi:10.1080/18811248.2011.9711675

[36] Z. Sun, W. L. Zhan, Z. Y. Guo, et al., Separation and Identification of Isotopes Produced from 20Ne+Be Reaction by Radioactive Ion Beam Line in Lanzhou. *Chin. Phys. Lett.* 15, 790 (1998). doi:10.1088/0256-307X/15/11/004

[37] Z. Sun, W. L. Zhan, Z. Y. Guo, et al., RIBLL, the radioactive ion beam line in Lanzhou. *Nucl. Instrum. Meth. A.* 503, 496–503 (2003). doi:10.1016/S0168-9002(03)01005-2

[38] J. W. Xia, W. L. Zhan, B. W. Wei, et al., The heavy ion cooler-storage-ring project (HIRFL-CSR) at Lanzhou. *Nucl. Instrum. Meth. A.* 488, 11–25 (2002). doi:10.1016/S0168-9002(02)00475-8

[39] W. L. Zhan, J. W. Xia, H. W. Zhao, et al., HIRFL Today. *Nucl. Phys. A.* 805, 533c–540c (2008). doi:10.1016/j.nuclphysa.2008.02.292

[40] S. Zhang, D. Niu, D. X. Wang, et al., Measurement of leakage neutron spectra for aluminium with D-T fusion neutrons and validation of evaluated nuclear data. *Fusion Eng. Des.* 171, 112582 (2021). doi:10.1016/j.fusengdes.2021.112582

[41] Q. Zhao, Y. Nie, Y. Ding, et al., Measurement and simulation of the leakage neutron spectra from Fe spheres bombarded with 14 MeV neutrons. *Nucl. Sci. Tech.* 34, 19–31 (2023). doi:10.1007/s41365-023-01329-6

[42] S. Zhang, Z. Chen, Y. Nie, et al., Measurement of leakage neutron spectra for Tungsten with D-T neutrons and validation of evaluated nuclear data. *Fusion Eng. Des.* 92, 41–45 (2015). doi:10.1016/j.fusengdes.2015.01.010

[43] S. Zhang, Z. Chen, R. Han, et al., Neutron Time Of Flight Spectrometer Based on HIRFL for Studies of Spallation Reactions Related to ADS Project. *Nucl. Sci. Tech.* 26, 84–87 (2015). doi:10.13538/j.1001-8042/nst.26.030502

[44] D. Satoh, S. Kunieda, Y. Iwamoto, et al., Development of SCINFUL-QMD Code to Calculate the Neutron Detection Efficiencies for Liquid Organic Scintillator up to 3 GeV. *J. Nucl. Sci. Technol.* 39, 657–660 (2002). doi:10.1080/00223131.2002.10875185

[45] X. Zhang, Z. Chen, R. Wada, et al., Thick target neutron yields from Beryllium, Carbon, Tungsten, and Lead targets irradiated by 26.7 MeV/nucleon 4He ions. *Nuclear Inst. and Methods in Physics Research, B.* 516, 48–54 (2022). doi:10.1080/00223131.2002.10875185

Figures

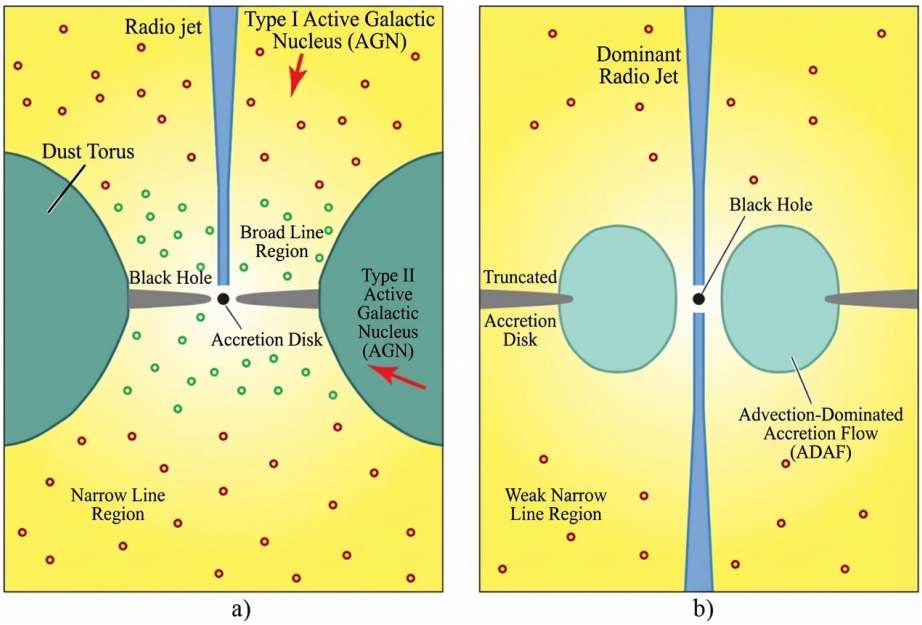

Figure 1: Figure 1